JOURNAL OF MATERIALS SCIENCE **39** (2004) 5259– 5262

Mechanism and kinetics of mechanically induced transformation of titanium and titanium hydride: Effect of reaction medium on microstructure, morphology and hydrogen-uptake properties

CH. BORCHERS
Institute of Material Physics, Göttingen University, Tammannstr.1, 37077 Göttingen, Germany

A. V. LEONOV
Lomonosov Moscow State University, Chemical Department, Leninskie Gory, 119899 Moscow, Russia

T. I. KHOMENKO, O. S. MOROZOVA*
Semenov Institute of Chemical Physics RAS, Kosygin St. 4, 119334 Moscow, Russia
E-mail: om@polymer.chph.ras.ru

The stimulating effect of graphite addition on hydrogen sorption/desorption properties of titanium activated under ball milling and titanium hydride activated or prepared under ball milling is studied using X-ray diffraction, scanning and transmission electron microscopy, and temperature-programmed reaction/desorption techniques. The formation of microporous carbon matrix containing randomly distributed titanium or titanium hydride fragments of several nm in size is found to be the major effect of graphite addition. This kind of morphology allows the hydrogen transport to titanium or from titanium hydride surfaces without hindrances and improves titanium–hydrogen interaction through modifying the titanium surface and subsurface layers by interstitial C atoms.

1. Introduction

High-energy ball milling is a low-cost and ecologically pure technique for metal-hydrides synthesis. Nowadays, this method is commonly used to prepare nanocrystalline Ti or Ti-hydride powders [1–3], which are promising for hydrogen storage applications. Graphite milled with metal powder improves the metal-to-hydrogen reactivity [4, 5]. The mechanism of such effect is poorly studied. However, this knowledge is important because of the actual interest in efficient hydrogen storage materials.

In this work, the stimulating effect of graphite addition on kinetics and mechanism of Ti-H_2 interaction induced by ball milling and on H_2 evolution from Ti-hydride activated or produced by ball milling is studied in detail.

2. Experimental

Elemental Ti powder (99.5% pure, $S = 0.01$ m^2/g) with spherical particles of $\sim$250 μm in diameter, TiH_2 (99% pure, 325 mesh, "Aldrich," $S = 0.32$ m^2/g), and pyrolytic graphite (99.0% pure, $S = 3$ m^2/g) were used. The milling treatments ($\sim$60 min) were carried out in a flow reactor (average energy intensity of 1.0 kW/kg) at room temperature and atmospheric pressure. The reactor was charged with 1.8 g of powder: Ti, TiH_2 or their mixture with graphite (0.3 g); the ball-to-sample ratio was 11. The outlet of the reactor was combined on-line with a gas chromatograph to test the effluent gases every 5–10 min. Before the milling started, the reactor was blown through with pure helium or a gas mixture of 64 vol% H_2/He. The flow rate was 0.008–0.01 l/min. The specific surface area (S) was measured with BET technique. XRD patterns were recorded by a Dron-3 diffractometer with Cu K_α anode. Morphological changes were studied by scanning (SEM), transition (TEM) and high-resolution transition (HRTEM) electron microscopy using a micro probe Cameca MBX-1M and a Philips EM 420 ST electron microscope. The TEM samples were prepared in an ethanol suspension and placed on copper grids covered by amorphous carbon. The sorption and evolution of H_2 were studied by temperature-programmed reaction (TPR) and temperature-programmed desorption (TPD) techniques in 6 vol% H_2/Ar or Ar flow (flow rate of 100 ml/min),

*Author to whom all correspondence should be addressed.

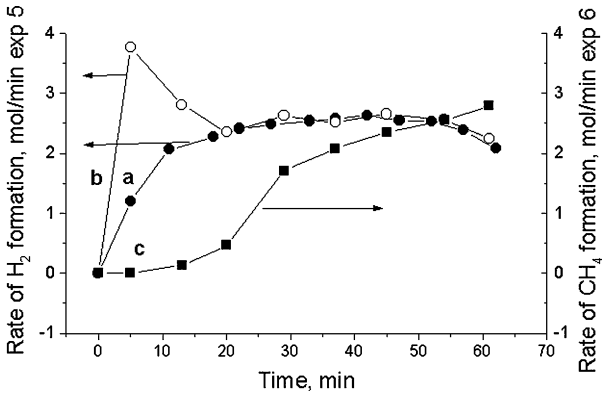

Figure 1 Kinetic curves of (a) H_2 evolution from TiH_2 and (b) H_2 evolution from TiH_2/graphite sample accompanied by (c) CH_4 formation under the milling in He flow.

on heating from 20 to 670°C with a heating rate of 10 K/min.

3. Results

3.1. Kinetics of Ti-H_2 interaction and TiH_2 decomposition

Fig. 1a shows H_2 evolution from TiH_2 under ball milling in He flow. The process started concurrently with milling. The milled sample lost $\sim 4.6 \times 10^{20}$ molecules H_2/g TiH_2 ($\sim$4 mol% of the total hydrogen content). During the ball milling, S increased from 0.32 to 6 m^2/g. Kinetics of H_2 evolution from TiH_2/C (Fig. 1b) is similar to that observed for TiH_2. Remarkable is the CH_4 formation detected after $\sim$10 min of milling. The CH_4 rate (Fig. 1c) progressively increases with milling time, which points to continuous mixing of TiH_2 and graphite [6]. The sample lost 7×10^{20} molecules H_2/g TiH_2 ($\sim$7 mol% of total hydrogen). For the final powder, $S = 38.2$ m^2/g.

Fig. 2a shows hydrogen sorption of pure Ti under the ball milling. The reaction starts after a short incubation period and is a stepwise process, which is typical for diffusion-controlled mechanisms. It means that the Ti-H_2 interaction virtually stops when reaction product (Ti-hydride) totally occupies the surfaces of Ti particles and starts again when the surface gets free. The

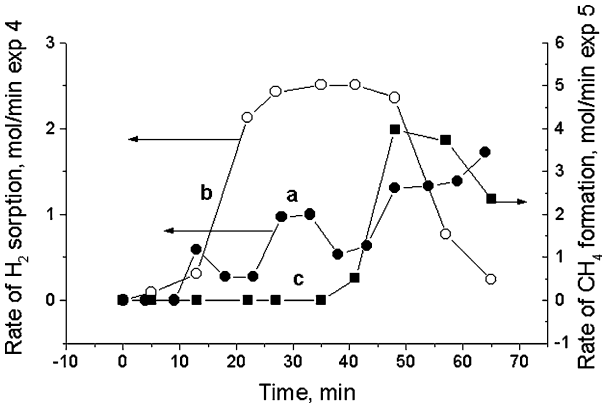

Figure 2 Kinetic curves of (a) H_2 sorption by Ti and (b) H_2 sorption by Ti/graphite samples accompanied by (c) CH_4 formation under the milling in 64 vol%H_2/He flow.

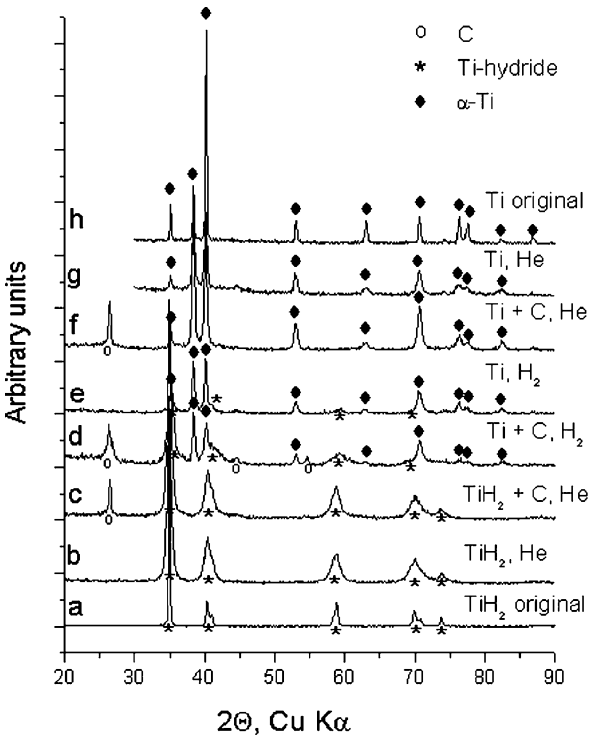

Figure 3 XRD patterns of TiH_2, TiH_2/graphite, Ti and Ti/graphite samples, original and after milling in He or 64 vol% H_2/He flow.

hydrogen sorption was $\sim 2 \times 10^{21}$ molecules H_2/g Ti. After the treatment, S increased from 0.01 to 1.9 m^2/g. Fig. 2b shows the dramatic change in kinetics of Ti-H_2 interaction caused by the graphite addition: hydrogen sorption proceeds without diffusion hindrances. CH_4 formation detected after 40 min of milling (Fig. 2c) is indicative to Ti-hydride formation [6]. The hydrogen sorption was $\sim 4 \times 10^{21}$ molecules H_2/g Ti. For the final powder, $S = 14.8$ m^2/g.

3.2. Structure and morphology of original and as-milled powders

Fig. 3 shows XRD spectra of original and as-milled powders. The original TiH_2 powder (Fig. 3a) consists of tetragonal phase of $TiH_{1.94}$ (JCPDS 26-983). The original Ti powder (Fig. 3h) consists of α-Ti (JCPDS 44-1294). XRD measurements of as-milled powders (including Ti and Ti/graphite powders milled during 60 in He flow) give the following results:

1. The treatment in He, see Fig. 3b and g, leads to a significant broadening of diffraction peaks of original TiH_2 and Ti due to crystalline size reduction and high strains. The fact that neither new peaks (except graphite) nor a shift in the TiH_2 and Ti diffraction peak positions were observed suggests that no significant dissolution of C into TiH_2 or Ti lattice occurs.

2. The treatment in H_2 leads to new diffraction peaks formation being attributed to Ti-hydride phases. As-milled Ti powder (Fig. 3d) contains $\sim$30 wt% of a tetragonal phase of Ti-hydride similar to that observed at $T < 310$ K ($a = 0.311$ nm, $c = 0.441$ nm, $c/a = 1.42$, average block size 10 nm). As-milled Ti/C powder contains 50–60 wt% of a cubic phase of $TiH_{1.6}$ [7] ($a = 0.441$ nm, average block size $\sim$6–7 nm). The α-Ti

lattice constants were similar to these of original Ti. The average block size was ~20 nm.

SEM measurements give the following results:

1. The original TiH_2 powder consists of particles with an average size of ~10 μm and rather smooth surfaces. After the milling in He, the major part of the powder consists of particles about 1–5 μm in size, the majority being on the small side. When graphite is added, the particle size falls to a few nm: small particles aggregate together to form larger particles with an average size of ~3 μm.

2. The original Ti powder consists of perfect spherical particles of narrow size distribution (~250 μm in diameter). The treatment in He or H_2 gives heterogeneous powders containing spherical particles, deformed spherical particles, and large flat platelets of ~300–400 μm in size with a smooth surface. A small fraction of fine powder, most probably, Ti-hydride, is observed after milling in H_2.

3. While graphite is added, the ball milling in He or in H_2, both results in powder size reduction to ~50 nm: particles of several μm in sizes lump together and only few large particles exist.

According to TEM, loose Ti-hydride particles of several hundreds nm in size, which consist of thin flakes stuck together, are quite typical for TiH_2 activated in He and Ti activated in H_2, respectively. The composite particles of 200–500 nm in size are quite typical for Ti/C and TiH_2/C milled samples. They consist of microporous carbon matrix with small Ti (Ti-hydride) fragments of 2–5 nm in size randomly distributed or 2–4 nm thick carbon and Ti (Ti-hydride) layers intermixed.

3.3. Hydrogen sorption-desorption properties

Fig. 4 shows TPD curves for original TiH_2 (Fig. 4a), as-milled TiH_2 (Fig. 4b) and as-milled TiH_2/C (Fig. 4c).

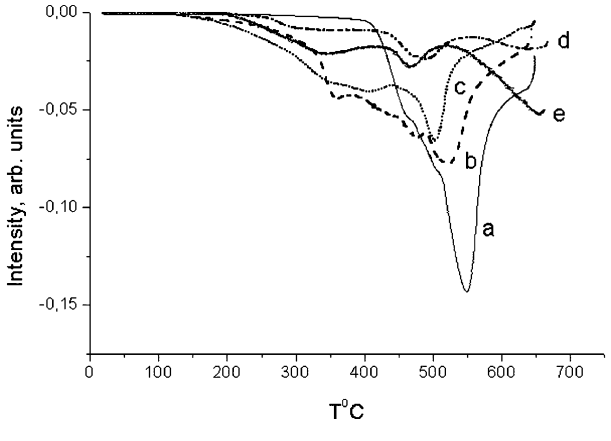

Figure 4 TPD of H_2 from TiH_2, TiH_2/graphite, Ti and Ti/graphite samples, original and milled in He or 64 vol% H_2/He flow: (a) TiH_2 original, (b) TiH_2 + He, (c) TiH_2/grahite + He, (d) Ti + 64 vol% H_2/He, and (e) Ti/graphite + 64 vol% H_2/He.

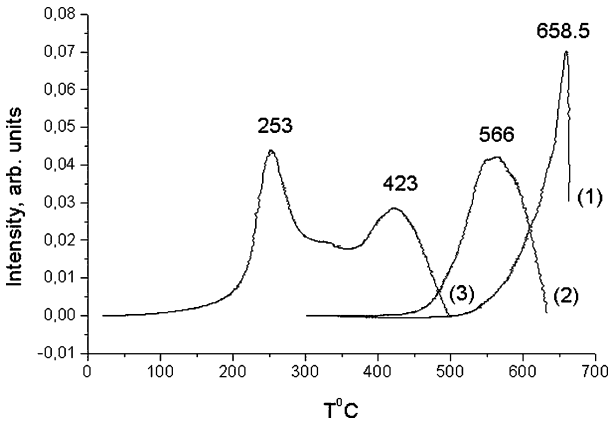

Figure 5 TPR of H_2 with Ti and Ti/ graphite samples, original and milled in He: (1)–Ti original; (2)–Ti milled in He and (3)–Ti/graphite milled in He.

For comparison, TPD spectra for Ti (Fig. 4d) and Ti/C (Fig. 4e) milled in H_2 are also given. Parameters of the TPD process are listed in Table I. The TPD curve for original TiH_2 has a single peak at $T_{max} = 541°C$. The TPD curve for as-milled TiH_2 has a very broad single peak shifted to low temperatures likely due to a high concentration of structural defects [8]. TPD spectra for TiH_2/C and Ti/C samples are characterized by the markedly larger low-temperature shift, two well divided TPD peaks instead of one broad peak, and by the hydrogen redistribution from the high-temperature peak to low-temperature peak. Similar features can be seen in TPR spectra of original Ti, as-milled Ti and as-milled Ti/graphite powders (Fig. 5). Parameters of TPR process are listed in Table II.

4. Discussion

In this work, two important experimental phenomena associated with the graphite addition were observed: (1) a strong increase in hydrogen sorption under milling conditions and (2) low-temperature sorption of H_2 of as-milled Ti samples and low-temperature decomposition of as-milled TiH_2. The first is likely to be caused by a change in mechanism of Ti-H_2 interaction through eliminating diffusion as the rate-determining factor. In this case, graphite works as a lubricant and anti-sticking agent, which eases the milling process (compare Fig. 2a and b) and helps to remove the reaction product (TiH_2) from the surface of Ti-particles. The result was observed by TEM as fine Ti-hydride fragments randomly distributed in a graphite matrix.

The reason of the second phenomenon is likely a decrease in Ti-H binding energy. In general opinion, hydrogen atoms occupy the tetrahedral interstitial sites in Ti lattice. Accordingly, the single-peak TPD and TPR curves for original TiH_2 and Ti (Figs 4a and 5a) exhibit one single type of hydrogen occupation site with a narrow energy distribution. The broadening of TPD and TPR peaks observed for as-milled TiH_2 and Ti may be attributed to continuous type of energy—site distribution caused by high concentration of structural defects detected by XRD and TEM. The two-peak TPD and TPR curves observed for as-milled TiH_2/graphite

TABLE I Effect of TiH_2 and Ti treatment on TPD parameters

Sample	Milling conditions	TPD: Ar, 10 K/min		
		T_{max} (°C)	H_2 (molecules/g Ti)	E_a(kJ/mol)
TiH_2 (Aldrich)	As-received	541	$\sim 1.1 \times 10^{22}$	~169
TiH_2 (1.5 g)	He flow, ~60 min	358–519	$\sim 9.4 \times 10^{21}$	131–164
TiH_2/graphite	He flow, ~60 min	~400	7.3×10^{21}	~140
(1.5 g + 0.3 g)		502	2.4×10^{21}	~161
Ti (1.5 g)	64 vol% H_2/He flow, ~60 min	340	8.2×10^{20}	~127
		488	1.17×10^{21}	~158
Ti/graphite	64 vol% H_2/He flow, ~60 min	343	2.6×10^{21}	~128
(1.5 g + 0.3 g)		465	1.2×10^{20}	~153

TABLE II Effect of Ti treatment on TPR parameters

Sample	Milling conditions	TPR: 6% H_2/Ar, 10 K/min		
		T_{max} (°C)	H_2 (molecules/g Ti)	E_a(kJ/mol)
Ti	As-received	658	2.7×10^{21}	~194
Ti (1.8 g)	He flow, ~60 min	566	4.2×10^{21}	~174
Ti/graphite	He flow, ~60 min	253	2.3×10^{21}	~37
(1.5 g + 0.3 g)		328	$\sim 1 \times 10^{20}$	
		423	7.6×10^{21}	~49

and Ti/graphite are the direct evidence for the creation of new types of hydrogen occupation sites. They are characterized by lower H_2 sorption and desorption activation energies (Tables I and II). The interstitial C atoms are most likely to be responsible for formation of these centers, because C atoms occupy the octahedral positions and disturb the neighboring tetrahedral positions suitable for hydrogen atoms [9]. The fact that no change in the lattice constants of as-milled TiH_2/C and Ti/C was observed (see Fig. 3) indicates that carbon atoms modify only the surface or subsurface layers of Ti (or Ti-hydride) particles. The process of modification is governed by intimate contact between graphite and Ti (Ti-hydride) surfaces, which was detected by TEM in the composite Ti/C and Ti-hydride/C particles.

5. Conclusions

The graphite related peculiarities of as-milled powder morphology are found to be responsible for (1) the elimination of diffusion control observed for the Ti-H_2 interaction, (2) an increase in titanium conversion to titanium hydride, and (3) a drastic decrease in the activation energy of H_2 sorption/desorption processes. Special type of sites with remarkably low Ti-H binding energy can be attributed to metal/graphite or hydride/graphite interfaces.

Acknowledgement

This work was partly supported by RFBR, project No. 01-03-32803.

References

1. H. ZHANG and E. H. KISI, *J. Phys. Condens. Matter* **9** (1997) L185.
2. D. A. SMALL, G. R. MACKAY and R. A. DUNLAP, *J. Alloys Compd.* **284** (1999) 312.
3. J.-L. BOBET, C. EVEN and J.-M. QUENISSET, *ibid.* **348** (2003) 247.
4. H. IMAMURA, Y. TAKESUE, S. TABATA, N. SHIGETOMI, Y. SAKATA and S. TSUCHIA, *Chem. Commun.* (1999) 2277.
5. S. BOUARICHA, J. P. DODELET, D. GUAY, J. HUOT and R. SHULZ, *J. Alloys Compd.* **325** (2001) 245.
6. C. BORCHERS, A. V. LEONOV and O. S. MOROZOVA, *J. Phys. Chem.* **106** (2002) 1843.
7. A. SAN-MARTIN and F. D. MANCHESTER, *Bull. Alloy Phase Diagr.* **8** (1987) 30.
8. O. S. MOROZOVA, A. N. STRELETSKII, I. V. BERESTETSKAYA, A. V. LEONOV and G. N. KRYUKOVA, *J. Metast. Nanocryst. Mater.* **8** (2000) 429.
9. Y. FUKAI, "The Metal-Hydrogen System. Basic Bulk Properties" (Springer Series in Material Science, Springer, Berlin, 1993) vol. 21.

Received 11 September 2003
and accepted 27 February 2004